THE TWO-STEP APPROACH FOR WHOLE-CORE RESONANCE SELF-SHIELDING CALCULATION

Shuai Qin[1], Qian Zhang[1*], Liang Liang[1], Qingming He[2] and Hongchun Wu[2]

[1] Harbin Engineering University
145 Nantong St, Harbin, Heilongjiang, 150001, China

[2]Xi'an Jiaotong University
No. 28 Xianning West Rd, Xi'an, Shaanxi, 710049, China

qinshuai@hrbeu.edu.cn, qianzhang@hrbeu.edu.cn, liangliang_ls@hrbeu.edu.cn, qingming_he@xjtu.edu.cn, hongchun@xjtu.edu.cn

ABSTRACT

A two-step approach is proposed to accomplish high-fidelity whole-core resonance self-shielding calculation. Direct slowing-down equation solving based on the pin-cell scale is performed as the first step to simulate different operating conditions of the reactor. Resonance database is fitted using the results from the pin-cell calculation. Several techniques are used in the generation of the resonance database to estimate multiple types of resonance effects. The second step is the calculation of practical whole-core problem using the resonance database obtained from the first step. The transport solver is embedded both at the first step and the second step to establish the equivalence relationship between the fuel rod in the practical problem and the pin-cell at the first step. The numerical results show that the new approach have capability to perform high-fidelity resonance calculations for practical problem.

KEYWORDS: resonance self-shielding; two-step approach; high-fidelity; whole-core

1. INTRODUCTION

The computing accuracy of the resonance self-shielding calculation is crucial in the high-fidelity direct whole-core calculation since the application of the method of characteristics (MOC) [1] is capable to give an acceptable error in the evaluation of spatial flux. Some advanced methods are proposed by the fusion of the equivalence theory [2] and the pin-based ultra-fine-group (UFG) [3] calculations to perform high-accuracy resonance self-shielding calculation [4-6]. The approach for the integration of the pin-based UFG calculation into the equivalence theory including two categories. The first one is the online calculation. In Ref. 4 and 5, the local resonance effects including the resonance interference effect and the intra-pin self-shielding are resolved by the online UFG calculations based on the quasi-1D cylindrical geometry [4] or the 2D pin-cell [5], along with the shadow effect is treated through the embedded self-shielding method (ESSM) [7] or the neutron current method (NCM) [8]. The computing accuracy of this type of approach is fully verified but it is reported in Ref. 9 that it suffers from efficiency loss in the depleted calculations for the whole-core due to the online pin-based UFG calculations. The second one is the heterogeneous resonance integral (RI) established by the pre-calculated pin-based UFG calculations [6]. The adoption of the heterogeneous RI in the depleted whole-core calculation can avoid low-efficiency

online UFG calculations. However, the intra-pin radial self-shielded XS is washed out in the heterogeneous RI, and the extra storage and the complicated multi-dimension interpolation will be brought by the consideration of the resonance interference in the heterogeneous RI.

In this study, a two-step approach is proposed to perform accurate and efficient resonance self-shielding calculations for whole-core problems. At the first step, the pin-based UFG calculations considering different operating conditions of the target core are performed to fit the resonance database (RD) instead of the heterogeneous RI. The polynomial fitting is adopted in the RD generation. And the accurate pin-level self-shielded XSs are evaluated directly by the fitted RD without excessive treatment. The modified ESSM equation is solved at both the two steps to establish the equivalence relationship between the actual fuel rod and the pin-cell case of the first step. The number density-perturbation technique [9] is adopted to resolve the resonance interference during the depletion, and a distributed parameter approach is developed to evaluate the intra-pin self-shielding. The methodology is introduced in Section 2 and the numerical tests are given in Section 3. The conclusions are given in Section 4.

2. METHODOLOGY

2.1. Generation Procedure of Resonance Database

In the generation of the RD, the pitch of the pin-cell is changed to cover the variation range of the background XSs of the actual rod in the target whole-core problem, and the ESSM is adopted to evaluate the background XS of designed pin-cell in the UFG calculations.

The ESSM equation as Eq. (1) is established for each resonant group based on the designed pin-cell. The fixed source is defined as the regional potential scattering XS and it is corrected by the IR parameter λ.

$$\vec{\Omega}\bullet\nabla\phi_g\left(\vec{r},\vec{\Omega}\right)+\left(\Sigma_{a,g}\left(\vec{r}\right)+\lambda\Sigma_{p,g}\left(\vec{r}\right)\right)\phi_g\left(\vec{r},\vec{\Omega}\right)=\frac{\lambda\Sigma_{p,g}\left(\vec{r}\right)}{4\pi} \tag{1}$$

Where $\Sigma_{p,g}$ and $\Sigma_{a,g}$ are the potential scattering XS and the absorption XS for group *g*, respectively. ϕ_g is the spatial flux.

Different from the original ESSM, the black assumption is adopted in the ESSM to enhance the computing accuracy of the two-step approach for the lattice with different types of fuel. The black assumption can be implemented by setting $\Sigma_{a,g}\left(\vec{r}\right)+\lambda\Sigma_{p,g}\left(\vec{r}\right)$ as a very large value like 10^6 and the background XS is calculated using Eq. (2):

$$\sigma_{b,g}=\frac{\left(\Sigma_{a,g}+\lambda\Sigma_{p,g}\right)^{\inf}\phi_f}{N_r} \tag{2}$$

Where N_r is the number density of resonant isotopes and ϕ_f is the flux in the fuel region.

The iterative process of original ESSM is eliminated in the black ESSM since the $\Sigma_{a,g}\left(\vec{r}\right)+\lambda\Sigma_{p,g}\left(\vec{r}\right)$ is set to a fixed value, and it is beneficial to improve the computing efficiency, especially for the whole-core calculation.

The number density-perturbation technique [9] is adopted as an efficient approach to treat the resonance interference effect in the depleted fuel. In the number density-perturbation technique, the assumption that the overall impact on the self-shielded XS of resonant isotopes can be decomposed into the product of

each impact brought by the individual perturbation of each resonant isotope is introduced and its validity is proven in Ref. 9. Based on this assumption, if we set the fuel composition under a certain burnup step as the base step, the self-shielded XS of isotope iso under any burnup can be written as:

$$\sigma_{iso} = \sigma_{iso}^{base} \prod_{k}^{N} R_k \tag{3}$$

Where N is the number of resonant isotopes in the mixture and R_k represents the ratio of the self-shielded XS of *iso* between the base state and the state that only perturb isotope k in the resonant mixture.

Based on the description above, the procedure for the generation of RD is described below:

(1) The pin-based depletion calculation is performed for each type of fuel to determine the base state and the perturbation state;
(2) Under the base state, a series of pin-based UFG calculation by changing temperatures and backgrounds (pin pitches) to obtain the accurate pin-level self-shielded XSs. Eq. (1) and (2) are solved by MOC on the design pin-cell geometry to evaluate the background XSs.
(3) For each grid of temperature and pin pitches (background XSs), the pin-based UFG calculations with perturbed composition are performed to determine the ratios of the self-shielded XS variations.
(4) The fitting procedure is performed using the results from the step (2) and (3). Polynomial fitting is adopted and the reference fitting form for the base state and the perturbation state are shown in Eq. (4) and (5), respectively.

$$\sigma_{base} = A_1T^2 + A_2T + A_3B^3 + A_4B^2 + A_5B + A_6B^2T + A_7BT \tag{4}$$

$$\begin{aligned} ratio = {} & A_1T^2 + A_2T + A_3B^3 + A_4B^2 + A_5B + A_6D^2 + A_7D \\ & + A_8BT + A_9DT + A_{10}BD \end{aligned} \tag{5}$$

(5) Step (2)-(4) are performed for all fuel types and the fitting coefficients are stored in the RD.

At the second step, the black ESSM equation is established for each group on the target problem with the base state of the fuel composition to evaluate the background XSs, and available for the calculation of self-shielded XSs in the base state using Eq. (4). Then the XSs are corrected by the perturbation of each resonant isotope using Eq. (5) to obtain the final self-shielded XSs.

2.2. Distributed Parameter Approach

A distributed parameter approach is proposed in this study to calculate the sub-ring self-shielded XSs which are washed out in the generation of RD. In fact, ^{238}U is the major resonant isotope in the LWR analysis and it has the most prominent rim effect, thus the treatment of the two-step approach for the intra-pin self-shielding mainly focuses on the ^{238}U. Ref. 10 has given an exponential-form radial distribution function for the ^{238}U RI in the fuel rod:

$$f(r) = a_0 + a_1 e^{a_2 (R-r)^{a_3}} \tag{6}$$

Where R is the outer radius of the fuel rod, and a_0, a_1, a_2, a_3 are called as the distributed (DRI) parameter. The value of the DRI parameter given in Ref. 10 is $(a_0 = 1, a_1 = 3, a_2 = -9.7, a_3 = 0.5)$. This DRI parameters are tested in Ref. 11 and the results show that it leads to the deviation in the radial calculation. A new set of DRI parameters $(a_0 = 1, a_1 = 5, a_2 = -13.0, a_3 = 0.5)$ is given Ref. 11 but its computing accuracy of the sub-ring self-shielded XS is still not satisfied with the new DRI parameter [5].

In this study, the non-line least-square fitting is adopted to evaluate the problem-dependent DRI parameters. Firstly, the distribution function is defined as:

$$f\left(r\right)=\frac{\sigma\left(r\right)}{\sigma_a}=a_0+a_1e^{a_2\left(R-r\right)^{a_3}} \tag{7}$$

Where $\sigma\left(r\right)$ represents the self-shielded XS of ^{238}U when the radius is *r*; σ_a represents the self-shielded XS of ^{238}U of the whole fuel rod.

In the generation of the RD, a certain number of the grids are selected for the radius, and the pin-based UFG calculation is performed to evaluate the self-shielded XS of these radius grids. The self-shielded XS of a certain radius grid is obtained by calculating the average XS of some differential element at this grid, that is, the self-shielded XS of radius r_1 could be evaluated using:

$$\sigma\left(r_1\right)\approx\bar{\sigma}\left(r_1+\Delta r\right) \tag{8}$$

And Δr must be very small, for example, 0.000001cm. The least-square problem can be established after obtaining the numerical set of the radius-XSs to calculate the problem-dependent DRI parameters:

$$\min\sum_{i=1}^{n}\left[\frac{\sigma\left(r_i\right)}{\sigma_a}-f\left(r_i\right)\right]^2 \tag{9}$$

Where *n* is the number of selected grids for the radius.

The Levenberg-Marquardt (LM) method [12] is adopted for the non-line least-square fitting. The self-shielded XS for a subring *i* can be written as Eq. (10) based on the assumption that the flux of the ring *i* can be regarded as a constant since its modest variation compared to the radial variation of the self-shielded XSs.

$$\begin{aligned}\sigma_{a,i}&=\int_{r_{i-1}}^{r_i}\sigma\left(r\right)\bar{\phi}_i r dr\Big/\int_{r_{i-1}}^{r_i}\bar{\phi}_i r dr\\&=\int_{r_{i-1}}^{r_i}\sigma_a f\left(r\right)\bar{\phi}_i r dr\Big/\int_{r_{i-1}}^{r_i}\bar{\phi}_i r dr\\&=\sigma_a g\left(\int_{r_{i-1}}^{r_i}f\left(r\right)r dr\Big/\int_{r_{i-1}}^{r_i}r dr\right)\end{aligned} \tag{10}$$

Where $\bar{\phi}_i$ is the flux in ring *i*.

To have a more intimate coupling with the generation of RD, the basic assumption is introduced in the distributed parameter approach: the ratio of the ^{238}U self-shielded XSs between the sub-ring and the whole fuel rod is constant along with the depletion. Therefore, it only needs the calculation of the DRI parameters for the base state. This assumption is tested on the UO_2 cell and MOX cell from the JAERI benchmark [13]. The direct UFG slowing-down calculation is performed to evaluate the self-shielded XSs with the fuel rod is divided into 10 rings with equal volume. Select a certain burnup step as the base state, and perform three different MOC transport calculation under each burnup step:

1) All the XSs are from the accurate sub-ring XSs obtained by the UFG calculations;

2) At base state, calculate the ratio of the XS between the sub-ring and the whole fuel rod, and the XSs of the sub-ring at other burnup steps are calculated by multiplying this ratio and the whole-rod XS at this burnup step;
3) At base state, calculate the ratio of the XS of ^{238}U between the sub-ring and the whole fuel rod, and the ^{238}U XSs of the sub-ring at other burnup steps are calculated by multiplying this ratio and the whole-rod XS at this burnup step. The XSs of the other resonant isotopes in the sub-ring are directly from its whole-rod XS.

The k-error is shown in Fig. 1 and two conclusions can be obtained: the first is that regardless of which burnup step is selected as the base state, the introduced k-error by the basic assumption of the distributed parameter approach is less than 20 pcm; the second is that the simplification that only consider the radial self-shielding of ^{238}U is reasonable, which brings less than 1.5/7 pcm of k-error for the UO_2/MOX cell.

Burnup step (GWd/t)

Base state (GWd/t)	0	0.1	5	10	15	20	30	50	70
0	0.00^{2-1} 0.32^{3-1} 0.32^{3-2}	-0.10^{2-1} 0.30^{3-1} 0.31^{3-2}	-2.73^{2-1} -2.32^{3-1} 0.41^{3-2}	-4.90^{2-1} -4.44^{3-1} 0.46^{3-2}	-6.57^{2-1} -6.09^{3-1} 0.48^{3-2}	-7.88^{2-1} -7.34^{3-1} 0.46^{3-2}	-9.56^{2-1} -9.16^{3-1} 0.40^{3-2}	-10.82^{2-1} -10.60^{3-1} 0.22^{3-2}	-10.88^{2-1} -10.80^{3-1} 0.08^{3-2}
0.1	0.01^{2-1} 0.32^{3-1} 0.31^{3-2}	0.00^{2-1} 0.31^{3-1} 0.31^{3-2}	-2.73^{2-1} -2.30^{3-1} 0.43^{3-2}	-4.89^{2-1} -4.43^{3-1} 0.46^{3-2}	-6.57^{2-1} -6.09^{3-1} 0.48^{3-2}	-7.87^{2-1} -7.40^{3-1} 0.47^{3-2}	-9.56^{2-1} -9.16^{3-1} 0.40^{3-2}	-10.82^{2-1} -10.58^{3-1} 0.24^{3-2}	-10.88^{2-1} -10.79^{3-1} 0.09^{3-2}
5	2.89^{2-1} 3.10^{3-1} 0.21^{3-2}	2.86^{2-1} 3.08^{3-1} 0.22^{3-2}	0.00^{2-1} 0.29^{3-1} 0.29^{3-2}	-2.30^{2-1} -1.97^{3-1} 0.33^{3-2}	-4.10^{2-1} -3.75^{3-1} 0.35^{3-2}	-5.51^{2-1} -5.15^{3-1} 0.36^{3-2}	-7.37^{2-1} -7.03^{3-1} 0.34^{3-2}	-8.89^{2-1} -8.66^{3-1} 0.23^{3-2}	-9.15^{2-1} -9.02^{3-1} 0.13^{3-2}
10	5.42^{2-1} 5.55^{3-1} 0.13^{3-2}	5.39^{2-1} 5.52^{3-1} 0.13^{3-2}	2.41^{2-1} 2.59^{3-1} 0.18^{3-2}	0.00^{2-1} 0.20^{3-1} 0.20^{3-2}	-1.90^{2-1} -1.67^{3-1} 0.23^{3-2}	-3.40^{2-1} -3.16^{3-1} 0.24^{3-2}	-5.40^{2-1} -5.17^{3-1} 0.23^{3-2}	-7.15^{2-1} -6.97^{3-1} 0.18^{3-2}	-7.57^{2-1} -7.45^{3-1} 0.12^{3-2}
15	7.56^{2-1} 7.61^{3-1} 0.05^{3-2}	7.54^{2-1} 7.58^{3-1} 0.04^{3-2}	4.47^{2-1} 4.52^{3-1} 0.05^{3-2}	1.98^{2-1} 2.04^{3-1} 0.06^{3-2}	0.00^{2-1} 0.08^{3-1} 0.08^{3-2}	-1.57^{2-1} -1.48^{3-1} 0.09^{3-2}	-3.71^{2-1} 3.60^{3-1} 0.11^{3-2}	-5.65^{2-1} -5.54^{3-1} 0.11^{3-2}	-6.23^{2-1} -6.13^{3-1} 0.10^{3-2}
20	9.38^{2-1} 9.36^{3-1} -0.02^{3-2}	9.36^{2-1} 9.34^{3-1} -0.02^{3-2}	6.23^{2-1} 6.15^{3-1} -0.08^{3-2}	3.67^{2-1} 3.58^{3-1} -0.09^{3-2}	1.63^{2-1} 1.55^{3-1} -0.08^{3-2}	0.00^{2-1} -0.06^{-1} -0.06^{3-2}	-2.24^{2-1} -2.27^{3-1} -0.03^{3-2}	-4.34^{2-1} -4.34^{3-1} 0.00^{3-2}	-5.05^{2-1} -5.02^{3-1} 0.03^{3-2}
30	12.08^{2-1} 11.95^{3-1} -0.13^{3-2}	12.07^{2-1} 11.91^{3-1} -0.16^{3-2}	8.87^{2-1} 8.56^{3-1} -0.31^{3-2}	6.23^{2-1} 5.86^{3-1} -0.37^{3-2}	4.10^{2-1} 3.72^{3-1} -0.38^{3-2}	2.38^{2-1} 2.01^{3-1} -0.37^{3-2}	0.00^{2-1} -0.32^{3-1} -0.32^{3-2}	-2.36^{2-1} -2.57^{3-1} -0.21^{3-2}	-3.26^{2-1} -3.40^{3-1} -0.14^{3-2}
50	15.11^{2-1} 14.79^{3-1} -0.32^{3-2}	15.08^{2-1} 14.75^{3-1} -0.33^{3-2}	11.88^{2-1} 11.18^{3-1} -0.70^{3-2}	9.19^{2-1} 8.32^{3-1} -0.87^{3-2}	6.97^{2-1} 6.04^{3-1} -0.93^{3-2}	5.17^{2-1} 4.24^{3-1} -0.93^{3-2}	2.63^{2-1} 1.75^{3-1} -0.88^{3-2}	0.00^{2-1} -0.70^{2-1} -0.70^{3-2}	-1.15^{2-1} -1.67^{2-1} -0.52^{3-2}
70	16.67^{2-1} 16.20^{3-1} -0.47^{3-2}	16.64^{2-1} 16.17^{3-1} -0.47^{3-2}	13.47^{2-1} 12.48^{3-1} -0.99^{3-2}	10.76^{2-1} 9.52^{3-1} -1.24^{3-2}	8.52^{2-1} 7.17^{3-1} -1.35^{3-2}	6.69^{2-1} 5.30^{3-1} -1.39^{3-2}	4.06^{2-1} 2.73^{3-1} -1.33^{3-2}	1.28^{2-1} 0.17^{3-1} -1.11^{3-2}	0.00^{2-1} -0.86^{3-1} -0.86^{3-2}

UO_2

Burnup step (GWd/t)

Base state (GWd/t)	0	0.1	5	10	15	20	30	50	70
0	0.00^{2-1} -6.34^{3-1} -6.34^{3-2}	-0.01^{2-1} -6.33^{3-1} -6.32^{3-2}	-1.76^{2-1} -7.94^{3-1} -6.18^{3-2}	-3.43^{2-1} -9.41^{3-1} -5.98^{3-2}	-4.93^{2-1} -10.71^{3-1} -5.78^{3-2}	-6.28^{2-1} -11.88^{3-1} -5.60^{3-2}	-8.60^{2-1} -13.79^{3-1} -5.19^{3-2}	-11.90^{2-1} -16.33^{3-1} -4.43^{3-2}	-13.82^{2-1} -17.50^{3-1} -3.68^{3-2}
0.1	0.01^{2-1} -6.33^{3-1} -6.34^{3-2}	0.00^{2-1} -6.32^{3-1} -6.32^{3-2}	-1.75^{2-1} -7.93^{3-1} -6.18^{3-2}	-3.43^{2-1} -9.41^{3-1} -5.98^{3-2}	-4.92^{2-1} -10.71^{3-1} -5.79^{3-2}	-6.27^{2-1} -11.86^{3-1} -5.59^{3-2}	-8.58^{2-1} -13.78^{3-1} -5.20^{3-2}	-11.89^{2-1} -16.32^{3-1} -4.43^{3-2}	-13.81^{2-1} -17.49^{3-1} -3.68^{3-2}
5	1.81^{2-1} -4.42^{3-1} -6.23^{3-2}	1.81^{2-1} -4.41^{3-1} -6.22^{3-2}	0.00^{2-1} -6.08^{3-1} -6.08^{3-2}	-1.71^{2-1} -7.61^{3-1} -5.90^{3-2}	-3.25^{2-1} -8.96^{3-1} -5.71^{3-2}	-4.64^{2-1} -10.16^{3-1} -5.52^{3-2}	-7.01^{2-1} -12.16^{3-1} -5.15^{3-2}	-10.41^{2-1} -14.82^{3-1} -4.41^{3-2}	-12.39^{2-1} -16.06^{3-1} -3.67^{3-2}
10	3.64^{2-1} -2.52^{3-1} -6.16^{3-2}	3.62^{2-1} -2.52^{3-1} -6.14^{3-2}	1.75^{2-1} -4.24^{3-1} -5.99^{3-2}	0.00^{2-1} -5.83^{3-1} -5.83^{3-2}	-1.58^{2-1} -7.23^{3-1} -5.65^{3-2}	-3.01^{2-1} -8.47^{3-1} -5.46^{3-2}	-5.43^{2-1} -10.54^{3-1} -5.11^{3-2}	-8.91^{2-1} -13.31^{3-1} -4.40^{3-2}	-10.96^{2-1} -14.64^{3-1} -3.68^{3-2}
15	5.34^{2-1} -0.70^{3-1} -6.04^{3-2}	5.33^{2-1} -0.71^{3-1} -6.04^{3-2}	3.41^{2-1} -2.50^{3-1} -5.91^{3-2}	1.62^{2-1} -4.14^{3-1} -5.76^{3-2}	0.00^{2-1} -5.59^{3-1} -5.59^{3-2}	-1.46^{2-1} -6.87^{3-1} -5.41^{3-2}	-3.94^{2-1} -9.00^{3-1} -5.06^{3-2}	-7.50^{2-1} -11.88^{3-1} -4.38^{3-2}	-9.60^{2-1} -13.28^{3-1} -3.68^{3-2}
20	6.94^{2-1} 0.99^{3-1} -5.95^{3-2}	6.92^{2-1} 0.99^{3-1} -5.93^{3-2}	4.96^{2-1} -0.86^{3-1} -5.82^{3-2}	3.12^{2-1} -2.54^{3-1} -5.66^{3-2}	1.48^{2-1} -4.03^{3-1} -5.51^{3-2}	0.00^{2-1} -5.36^{-1} -5.36^{3-2}	-2.54^{2-1} -7.56^{3-1} -5.02^{3-2}	-6.18^{2-1} -10.53^{3-1} -4.35^{3-2}	-8.32^{2-1} -12.01^{3-1} -3.69^{3-2}
30	9.82^{2-1} 4.09^{3-1} -5.73^{3-2}	9.82^{2-1} 4.09^{3-1} -5.73^{3-2}	7.76^{2-1} 2.13^{3-1} -5.63^{3-2}	5.86^{2-1} 0.35^{3-1} -5.51^{3-2}	4.15^{2-1} -1.21^{3-1} -5.36^{3-2}	2.62^{2-1} -2.60^{3-1} -5.22^{3-2}	0.00^{2-1} -4.91^{3-1} -4.91^{3-2}	-3.77^{2-1} -8.07^{3-1} -4.30^{3-2}	-6.00^{2-1} -9.68^{3-1} -3.68^{3-2}
50	14.30^{2-1} 9.02^{3-1} -5.28^{3-2}	14.29^{2-1} 9.02^{3-1} -5.27^{3-2}	12.12^{2-1} 6.89^{3-1} -5.23^{3-2}	10.10^{2-1} 4.98^{3-1} -5.12^{3-2}	8.31^{2-1} 3.28^{3-1} -5.03^{3-2}	6.70^{2-1} 1.79^{3-1} -4.91^{3-2}	3.94^{2-1} -0.73^{3-1} -4.67^{3-2}	0.00^{2-1} -4.19^{2-1} -4.19^{3-2}	-2.36^{2-1} -6.00^{2-1} -3.64^{3-2}
70	17.18^{2-1} 12.37^{3-1} -4.81^{3-2}	17.18^{2-1} 12.37^{3-1} -4.81^{3-2}	14.90^{2-1} 10.12^{3-1} -4.78^{3-2}	12.82^{2-1} 8.09^{3-1} -4.73^{3-2}	10.98^{2-1} 6.31^{3-1} -4.67^{3-2}	9.32^{2-1} 4.73^{3-1} -4.59^{3-2}	6.48^{2-1} 2.07^{3-1} -4.41^{3-2}	2.43^{2-1} -1.59^{3-1} -4.02^{3-2}	0.00^{2-1} -3.57^{3-1} -3.57^{3-2}

MOX

Figure 1. Error of k-infinity

3. NUMERICAL RESULTS

In this section, the assembly problems, a multi-assembly problem and a multicell lattice are tested for verification. The direct UFG slowing-down calculation and the MCNP 5 [14] tallying are adopted for the reference calculations. The wims-69 group is employed in the calculation and group 15^{th} -27^{th} is the resont groups. The CPU for the calculation is Intel®, Core™ i7-7700HQ, 2.8GHz.

3.1 PWR Assembly

The two-step approach calculations are performed for the UO_2 and the MOX assembly from the JAERI benchmark [13]. The ray conditions for the self-shielding calculations of the UO_2/MOX assembly are 32/8 azimuthal angles in the first quadrant, 80/20 rays in each direction and 8/8 polar angles with GL quadrature set. The reference results are obtained by the direct UFG calculations.

The burnup calculation is also performed by HELIOS 1.7 code [15]. The fuel composition under 15 GWd/t is specified as the base state, and the setting of the perturbation state covers the variation of the fuel compositions from 0 to 70 GWd/t. The identical 69-group MOC transport calculation is performed using the self-shielded XSs evaluated by the two-step approach and the reference calculation,

respectively. The MOC ray conditions in the transport calculation are 8 azimuthal angles, 20 rays in each direction and 8 polar angles with GL quadrature set for both the UO_2 assembly and the MOX assembly.

Fig. 2 is the distribution of relative errors over burnup steps for the self-shielded XSs of the UO_2 assembly and MOX assembly. Table I is the error of k-infinity during burnup. It can be seen form Fig. 2 that higher errors are introduced in the Gd bearing fuel rod and the UO_2 rod around the Gd rod. These results are attributed to it that the inconsistency between the pin-cell in uniform lattice for the RD generation and the fuel rod in the assembly is enhanced because the strong neutron absorption of Gd. However, the self-shielded XSs evaluated by the two-step approach still have a good agreement with the reference results. The RMS errors of ^{238}U self-shielded XSs in the UO_2 fuel pin, the Gd fuel pin and MOX fuel pin are less than 0.67%, 1.51% and 0.25%, respectively. The k-error brought by the self-shielded XSs are less than 63.0 and 73.3 pcm for the UO_2 and MOX assembly, respectively.

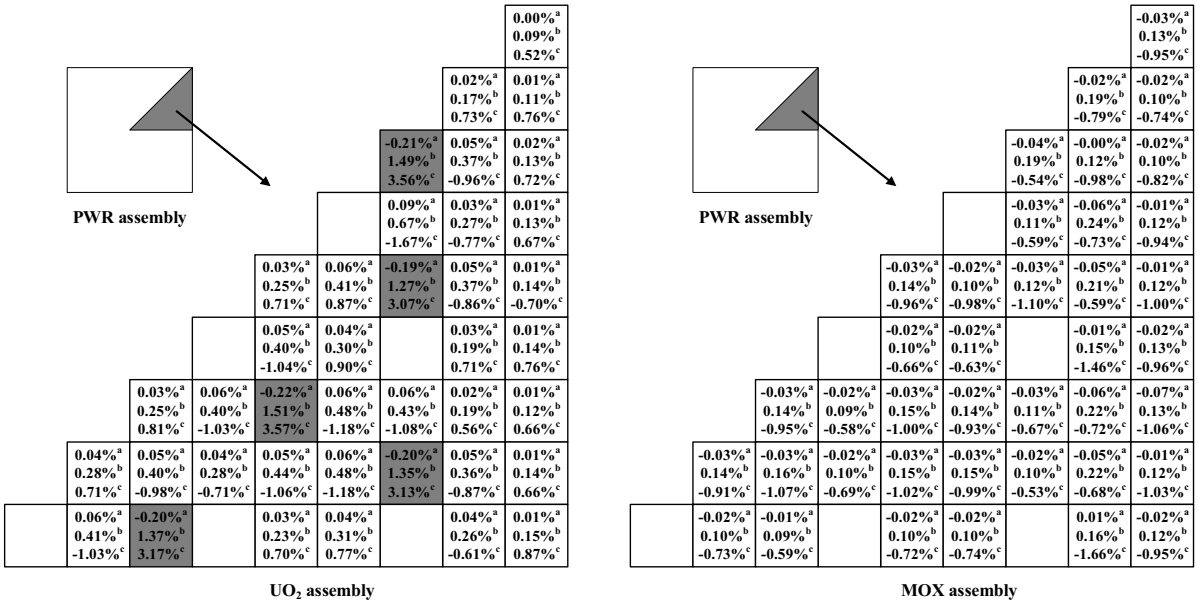

a: Average error of self-shielded XSs; b: RMS error of self-shielded XSs; c: Maximum error of ^{238}U self-shielded XSs.

Figure 2. The Distribution of Relative Errors over Burnup Steps for Self-Shielded XSs

Table I. K-Error during Burnup

Burnup (GWd/t)	0	0.1	5	10	15	20	30	50	70
k error(pcm)-UO_2	62.2	62.3	54.4	44.1	43.1	49.2	63.0	57.4	39.5
k error(pcm)-MOX	73.3	73.2	70.1	68.0	66.7	65.7	65.8	66.3	68.3

3.2 Multi-Assembly Problem

A multi-assembly problem designed on C5G7 geometry [16] is used to test the ability of the two-step approach for the whole-core calculation. The material specification is specific in Ref. 17

The MOC ray conditions for the self-shielding calculation are 6 azimuthal angles in the first quadrant, 30 rays in each direction and 16 polar angles with GL quadrature set. The MCNP 5 tallying with 300 batches (50 inactive batches) and 10 000 000 particles per batch is performed for reference. Fig. 3 is the distribution of RMS relative errors of self-shielded XSs. From the data in Fig. 3, it can be seen that the maximum RMS error is less than 1%. The identical 69-group MOC calculations are performed using the self-shielded XSs from the two-step approach and the MCNP tallying. The MOC ray conditions for the transport calculation are 8 azimuthal angles in the first quadrant, 20 rays in each direction and 8 polar

angles with GL quadrature set. Table II gives the k-infinity comparison and error introduced by the self-shielding calculation is -30.6 pcm.

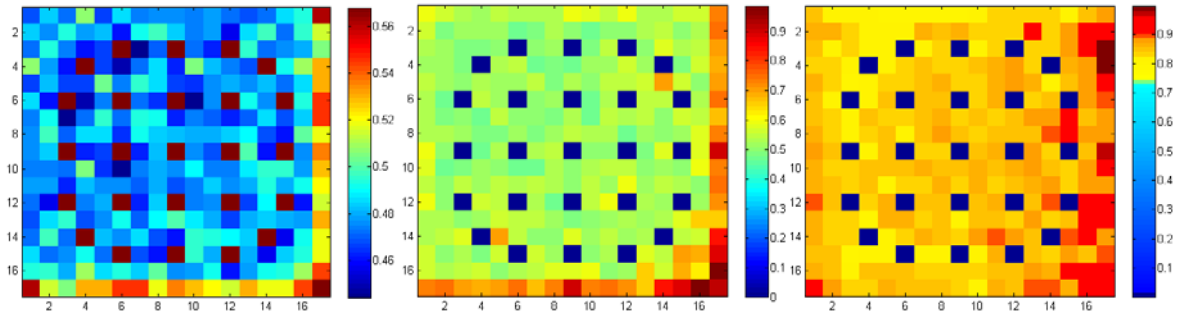

(a) **(b)** **(c)**

a: Inner UO_2 assembly; b: outer UO_2 assembly; c: MOX assembly

Figure. 3 The Distribution of RMS Relative Errors of Self-Shielded XSs

Table II. The Comparison of K-Infinity in Multi-Assembly Problem

	MOC-Reference	MOC-Two-step scheme	Error (pcm)
k-infinity	1.324493	1.324187	-30.6

3.3 Test for Intra-Pin Self-Shielding

A self-design 3×3 multicell lattice shown in Fig. 4 is used to test the accuracy of the distributed parameter approach on the evaluation of intra-pin self-shielding. The material specifications are from the UO_2 cell in JAERI benchmark and the fuel rod is divided into 10 rings with equal volume. 300 batches (50 inactive batches) with 3 000 000 particles per batch is used for MCNP 5 tallying to calculate the reference results.

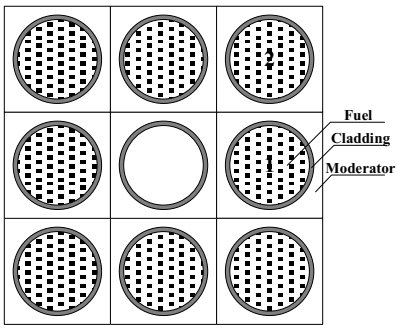

Pellet outer diameter: 0.824cm
Cladding outer diameter: 0.952cm
Fuel rod distance: 1.265cm

Figure. 4 Geometric Configuration And Parameter of Multicell Lattice

The pin-level self-shielded XSs used for the evaluation of intra-pin self-shielding are obtained by the two-step approach, and the conditions for MOC ray generation are: 32 azimuthal angles in the first quadrant; 80 rays in each direction; 8 polar angles with GL quadrature set. Fig. 5 and 6 give the comparison of intra-pin self-shielded XSs of group 24^{th} and 27^{th} in the fuel rods marked in Fig. 4. It can be observed that the maximum relative error is less than 1%. The identical 69 group MOC transport calculation for the lattice is performed using the self-shielded XSs obtained by the two-step scheme and MCNP tallying, respectively. The comparison of k-infinity is tabulated in Table III and it can be seen that the k-error introduce by the self-shielding calculation is 16.7 pcm

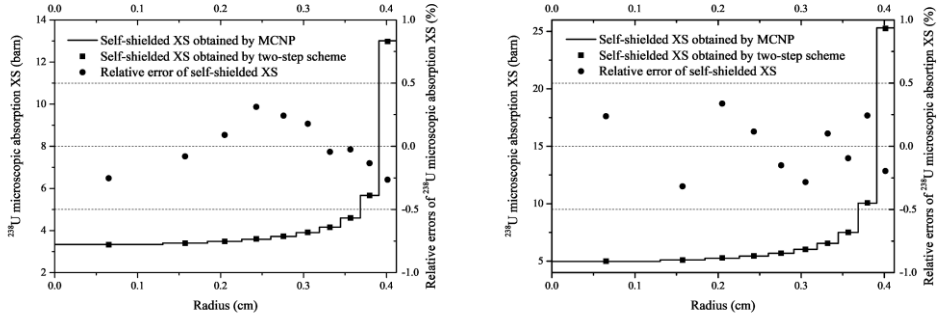

Figure. 5 The Comparison Of ^{238}U Microscopic Absorption XS in No.1 Rod

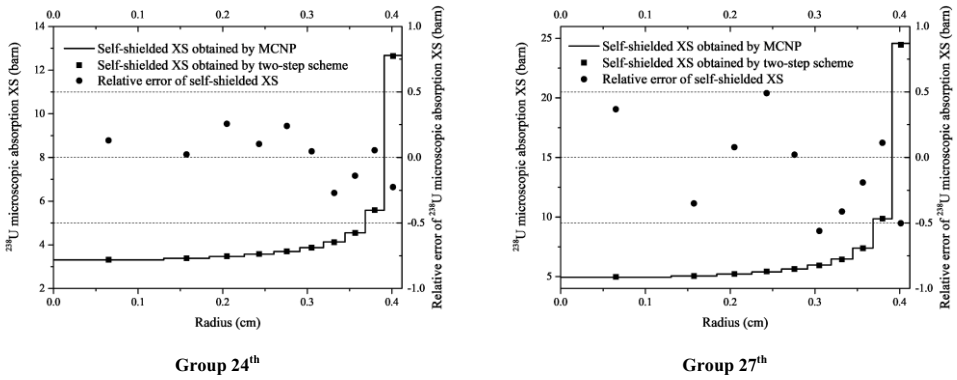

Figure. 6 The Comparison Of ^{238}U Microscopic Absorption XS in No.2 Rod

Table III. Comparison of K-Infinity

	MOC-MCNP	MOC-two-step scheme	Error (pcm)
k-infinity	1.460434	1.460601	16.7

4. CONCLUSIONS

A new resonance self-shielding method named the two-step approach is proposed to accomplish the high-fidelity whole-core resonance self-shielding calculation. At the first step, the pin-based UFG calculations are performed to fit the RD. At the second step, the self-shielding calculation of the target whole-core problem is performed using the RD generated before. The black-assumption ESSM is adopted to establish the equivalence relationship between the designed pin-cell and the actual fuel rod in the target problem. And the number density-perturbation technique is adopted to resolve the resonance interference in depleted fuel. A distributed parameter approach is proposed to evaluate the intra-pin sub-ring self-shielded XS which is washed out in the original RD. Multiple problems are calculated to test the ability of the two-step approach, and the numerical results show that the two-step approach can achieve the same level of computing accuracy as the direct UFG calculation and the MCNP tallying.

ACKNOWLEDGMENTS

This work is supported by the fund provided by the following sources: Heilongjiang Province Science Foundation for Youths [QC2018003]; Fundamental Research Funds for the Central Universities [grant numbers GK2150260178]

REFERENCES

1. J.R. Askew, 1972. *A characteristics formulation of the neutron transport equation in complicated geometries* (No. AEEW-M--1108). United Kingdom Atomic Energy Authority.
2. R.J. Stamm'ler and M.J. Abbate, 1983. *Methods of steady-state reactor physics in nuclear design* (Vol. 111). London: Academic Press.
3. P.H. Kier and A.A. Robba, 1967. *RABBLE: A PROGRAM FOR COMPUTATION OF RESONANCE ABSORPTION IN MULTIREGION REACTOR CELLS* (No. ANL-7326). Argonne National Lab., Ill.
4. Y. Liu, W. Martin, M. Williams and K.S. Kim, 2015. A full-core resonance self-shielding method using a continuous-energy quasi–one-dimensional slowing-down solution that accounts for temperature-dependent fuel subregions and resonance interference. *Nuclear Science and Engineering*, **180**(3), pp.247-272.
5. S. Choi, A. Khassenov and D. Lee, 2016. Resonance self-shielding method using resonance interference factor library for practical lattice physics computations of LWRs. *Journal of Nuclear Science and Technology*, **53**(8), pp.1142-1154.
6. Q. Zhang, Q. Zhao, Z. Zhang, L. Liang, W. S. Yang, H. Wu and L. Cao, 2018. Improvements of the Embedded Self-Shielding Method with Pseudo-Resonant Isotope Model on the Multifuel Lattice System. *Nuclear Science and Engineering*, **192**(3), pp.311-327.
7. S.G. Hong and K.S. Kim, 2011. Iterative resonance self-shielding methods using resonance integral table in heterogeneous transport lattice calculations. *Annals of Nuclear Energy*, **38**(1), pp.32-43.
8. N. Sugimura and A. Yamamoto, 2006. Evaluation of Dancoff factors in complicated geometry using the method of characteristics. *Journal of nuclear science and technology*, **43**(10), pp.1182-1187.
9. Q. Zhang, Q. Zhao, W.S. Yang and H. Wu, 2018. Modeling of Resonance-Interference Effect in Depleted Fuel Compositions by Pseudo Resonant Isotopes. *Nuclear Science and Engineering*, **191**(1), pp.46-65.
10. I.D. Palmer, K.W. Hesketh and P.A. Jackson, 1982, March. A Model for Predicting the Radial Power in a Fuel Pin. *In IAEA Specialist Meeting on Fuel Element Performance Computer Modeling* (pp. 15-19).
11. Z. Xu, J. Rhodes and K. Smith, 2009, May. CASMO-5 versus MCNP-5 benchmark of radial power profile in a fuel pin. *In International Conference on Mathematics, Computational Methods & Reactor Physics (M&C)*. Saratoga Springs, NY, USA.
12. D.W. Marquardt, 1963. An algorithm for least-squares estimation of nonlinear parameters. *Journal of the society for Industrial and Applied Mathematics*, **11**(2), pp.431-441.
13. A. Yamamoto, T. Ikehara, T. Ito and E. Saji, 2002. Benchmark problem suite for reactor physics study of LWR next generation fuels. *Journal of Nuclear Science and Technology*, **39**(8), pp.900-912.
14. X-5 Monte Carlo Team, 2003. *MCNP—A General N-Particle Transport Code, Version 5—Volume I: Overview and Theory*. LA-UR-03-1987, Los Alamos National Laboratory.
15. R.J. Stamm'ler, 2003. *HELIOS Methods*. Studsvik Scandpower.
16. E.E. Lewis, M.A. Smith, N. Tsoulfanidis, G. Palmiotti, T.A. Taiwo and R.N. Blomquist, 2001. Benchmark specification for Deterministic 2-D/3-D MOX fuel assembly transport calculations without spatial homogenization (C5G7 MOX). *NEA/NSC*, 280.
17. S. Cathalau, J.C. Lefebvre and J.P. West, 1996. Proposal for a second stage of the Benchmark on Power Distributions within Assemblies, an earlier version of the published OECD/NEA benchmark. *NEA/NSC/DOC* (96) 2, Nuclear Energy Agency.